Comparison of dynamic models for a DC railway electrical network including an AC/DC bi-directional power station

Khaled Almaksour, Youssef Krim, N'guessan Kouassi, Nicolas Navarro, Bruno François, Tony Letrouvé, Christophe Saudemont, Lionel Taunay, Benoit Robyns

Version of Record: https://www.sciencedirect.com/science/article/pii/S0378475420301865
Manuscript_98116e57c3117f8b11c088776ce1c06f

Comparison of dynamic models for a DC railway electrical network including an AC/DC bi-directional power station

Khaled Almaksour(1), Youssef Krim(1), N'guessan Kouassi(1)(2), Nicolas Navarro(2), Bruno François(1), Tony Letrouvé(4), Christophe Saudemont(1), Lionel Taunay(3) and Benoit Robyns(1)

(1) Univ. Lille, Arts et Metiers Institute of Technology, Centrale Lille, Yncrea Hauts-de-France, ULR 2697 – L2EP, F-59000 Lille, France
(2) Railenium, 180 rue Joseph-Louis Lagrange, 59300 Famars, France
(3) SNCF Réseau, 6 Avenue François Mitterrand, 93574 La Plaine Saint Denis, France
(4) SNCF- Direction Innovation & Recherche, 1-3 Avenue François Mitterrand, 93574 La Plaine Saint Denis, France
Corresponding author: Khaled Almaksour, E-mail: khaled.almaksour@yncrea.fr

Abstract - To face environmental issues, SNCF, the French railway, has chosen to improve the energy efficiency of its electrical power system by investigating solutions for regenerative braking. With the contribution of Railenium, a research and test center in railway activities, they aim to recover the braking energy by setting up a reversible inverter in the DC substation "Masséna". The issue is to test, implement and compare various control solutions to increase the energy efficiency with minimum impacts on the railway operation. In this paper, a simulation model for studying a reversible power substation is addressed by considering AC and DC equivalent electrical sources. The proposed model provides a reliable tool for analyzing the behavior of the railway electrical network during specially braking mode. In order to validate this model, its simulation results are compared with the ones obtained from Esmeralda, the SNCF professional software. A first configuration is led without the inverter and gives certified Esmeralda results and validates the proposed model despite some gaps in powers and voltages due to differences in input data and models. A second comparison with inverter is presented to highlight the main difference between the proposed model and Esmeralda. In addition, laboratory experimental activities are put forward to investigate the proposed model by using power-hardware-in-the-loop simulations. Finally, a simulation test under MATLAB software with fifty train's traffic is presented to estimate the energy saving thanks to the installed inverter. For this latter case study, the system sent back to the national AC grid around 6.9% of the total energy consumed by all trains.
Keywords- Railway system; dynamic model; Regenerative power; Real time simulation; Power-Hardware-In-the-Loop

1. Introduction

Global warming and the scarcity of energy resources have led transport activities and companies to find ways of reducing their carbon footprint and their energy consumption [1-2]. Improving the energy efficiency has become an important challenge in railway electrical systems [3-4]. In this context, the French national railway company SNCF intends to put in place technical solutions that allow the control and the optimization of energy consumption. The main means to do this is the use of regenerative braking.
Since 1970, electric vehicles with braking energy recovery have been explored [5]. In the braking phase of the train, the recovered energy obtained is used to supply the auxiliary loads (heating, lighting, air-conditioning) or/and can be reinjected into the catenary [6]. During this operation phase, the electromechanical torque of their motors becomes smaller than the braking torque. Therefore, the machine torques become negative and makes operate the machines in the generator mode to produce power. This power is called regenerative braking power. In this work, the rolling stock is supplied by rectifier-based substations with 1.5 kV DC. The drawback of this DC system concerns braking energy, which cannot be returned to the main grid if it is not consumed on the railway network. If there is no train in traction and no load on the system to absorb this regenerative energy, the voltage of the DC catenary increases [6]. To overcome this problem, some strategies can either be involved: to optimize

the train's operations [7-8] (optimization timetables, efficient energy based driving) or to address an updating of the railway power network by integrating new hardware equipment such as energy storage [9]. Train timetable optimization has been suggested as one of the approaches to increase the recuperation ratio of the regenerative braking energy. In this technique, the acceleration and braking actions of two neighboring trains are scheduled to occur simultaneously. Thus, the train in traction mode uses some of the produced energy by the train in deceleration. Some studies demonstrate that up to 14% of energy saving can be recuperated through the timetable synchronization [10]. Energy Storage System (ESS), if properly sized, can absorb the energy provided by a braking train and give it back when needed to supply other trains in acceleration [11]. Many examples of real world implementation of on-board ESS are given in the literature. Brussel metro and tram lines and Madrid Metro line in Europe show 18.6% - 35.8% and 24% energy saving in respectively [12-13-14]. Another solution is to capture this energy by installing a reversible AC/DC piloted inverter. SNCF has decided to investigate this latter solution.
A comparative analysis between different braking recuperation techniques is presented in table 1 to position the solution proposed in this study in relation with the literature.

Table I. Comparative framework between different recuperation methods

Energy Recuperation technique	**Advantages**	**Disadvantages**	**References**
Onboard ESS	- Possible operation without catenary, -Reduces voltage drops, -Increases efficiency and reduces third rail losses, -Possible to control of the DC voltage,	-High cost due to installation of ESS on the train, -Power management is needed to control the maximum and minimum limit of the capacity, -Elevated security constraints due to onboard passengers, -lifespan influenced by the number of charge / discharge cycles, -Standstill vehicles for repair and maintenance,	[13] [15]
Wayside ESS	-Can be used by all trains running on the line, -Implementation between substations, -Repair and maintenance do not effect trains operation, -Possible to control of the DC voltage,	- Increases overhead line losses because of the release and absorption of energy on the traction line, -Power management is needed to control the maximum and minimum limit of the State of Charge (SoC) of the storage system, -Analysis is needed for choosing the favorable location and sizing, -lifespan influenced by the number of charge / discharge cycles,	[16] [17] [18]
Synchronization time	-Possible application of Artificial Intelligence, - Low cost,	-Analysis is needed for speed profile and timetable,	[19]
Reversible substation	-Repair and maintenance do not affect the train operation, -Electricity can be sold to the electricity market, -Possible to control of the DC voltage, -Can be used by all trains moving on the line, -Lower safety constraints,	-Analysis is needed for choosing the favorable location,	Treated in this article [6] [20]

Many recent researches have investigated in the modeling and simulation of electrical railway systems. Ref. [21] considers that the application of a simplified model based on a perfect DC voltage

source in series with a resistance is adapted to model the substation. Ref. [22] presents a model of a train including an on-board hybrid accumulation system to be used in DC traction networks. Ref. [6] proves using simulation tests of a DC railway system model that a reversible inverter can participate to share regenerative braking power among multiple traction substations. Ref [23] illustrates the performance of a DC electric rail transit system model, which includes trains, substations, rail systems and braking regenerative system. In this context, this paper presents a detailed dynamic model for complete railway electrical network including an AC/DC bidirectional substation based on a power converter in order to increase the accuracy of the results from the simulation. The using of the modern solutions based on power electronics offers attractive performance. The valuation of the developed model is carried out using Esmeralda software and experimental implementation using power-hardware-in-the-loop simulations. Esmeralda is a calculation software developed by SNCF for its own needs. It simulates rail dynamics by taking into consideration the characteristics of trains as well as the electrical network structure. The simulations carried out under Esmeralda allow SNCF, among other uses, to size and choose the right location of the substations, to estimate the consumption of the rail power network and to assess its economic and technical performances [24]. Despite the services provided by Esmeralda, there remains a black box inaccessible for research and development field. It is therefore necessary to reconstruct the accessible dynamic model in order to formulate the problem of recovering braking energy by incorporating a controlled inverter to improve the energy efficiency, while ensuring better electrical performance (mainly voltage level).
Indeed, the DC power substation named "Masséna" in Paris will be made reversible by adding an inverter. This inverter will send back the regenerative braking energy to the AC upstream HV network. A precise model of the power railway system is needed in order to investigate the optimization of power flows in the power system. This paper presents the modeling of the railway power network involving the reversible "Masséna" substation and its two neighboring substations "Les Ardoines" and "Quai de la Gare".
The paper is organized as follow: A description of the studied electrical railway network is presented in Section 2. The proposed model with the inverter added in "Masséna" substation is detailed in Section 3. Simulation results of the proposed model are presented in Section 4 which is divided in three subsections; the first one shows a validation and comparison of the results obtained by the proposed model with the ones obtained by Esmeralda software. The second subsection provides results of real-time simulation of the proposed model using Power-Hardware-In-the-Loop concept with a real laboratory power scaled inverter. In the third subsection, a case study of the energy gain obtained with the "Masséna" inverter is presented with simulation results for one-hour traffic. A conclusion is finally conducted in Section 5.

2. Description of the studied electrical railway network

Currently in France, the majority of the railway system is mainly powered by 1500 V DC and 25 kV/50 Hz single-phase electrified lines [25]. Starting from a high voltage energy distribution, the substations carry out transformers (lowering voltage) and diode rectifiers (AC/DC conversion) to distribute the current, via the catenary and the pantograph, to the rolling stock [26]. Single-phase catenaries supply is realized by transforming the high voltage drawn between two phases of the three-phase transmission network (63 kV, 90 kV, 225 kV, 400 kV) to a voltage of 25 kV [25]. The SNCF rolling stock comes from the Z2N multiple unit class. They are powered under two voltage levels: 25 kV/50 Hz or 1.5 kV DC [27]. Trains using this equipment can be in a single unit or in a multiple unit. A single unit consists of four cars: two motorized cars and two passengers' cars.
In the particular case of the "Masséna" project, three electrical traction substations located on the railway line C of the Paris RER are studied: "Quai de la Gare", "Masséna" and "Les Ardoines". As shown in Fig. 1, "Masséna" and "Les Ardoines" are supplied by the national high voltage transmission grid at 63 kV AC and contain two traction groups operating alternately. While "Quai de La Gare" substation has three traction groups, two of them are connected to the catenary and the third one is used in case of emergency. The substations are equipped with diode rectifiers supplied by transformers. The rectifier with the associated transformer compose the traction unit, which ensures the power conversion from upstream AC grid to the DC catenary. The trains are powered by direct current, via the 1500 V catenary. The substation location and trains position are defined by using P_k

(kilometric point) value which provides reference points alongside the railway line. The considered railway section starts at "Quai de la Gare" substation (P_k =0.975 km) and ends at "Les Ardoines" substation (P_k=6.8 km). "Masséna" substation is located in between with P_k=2.495 km. Moreover, the "Masséna" substation hosts a new 1 MW inverter and its associated transformer. This inverter, currently under test, will only be dedicated for pathing braking power from braking trains to the AC grid.

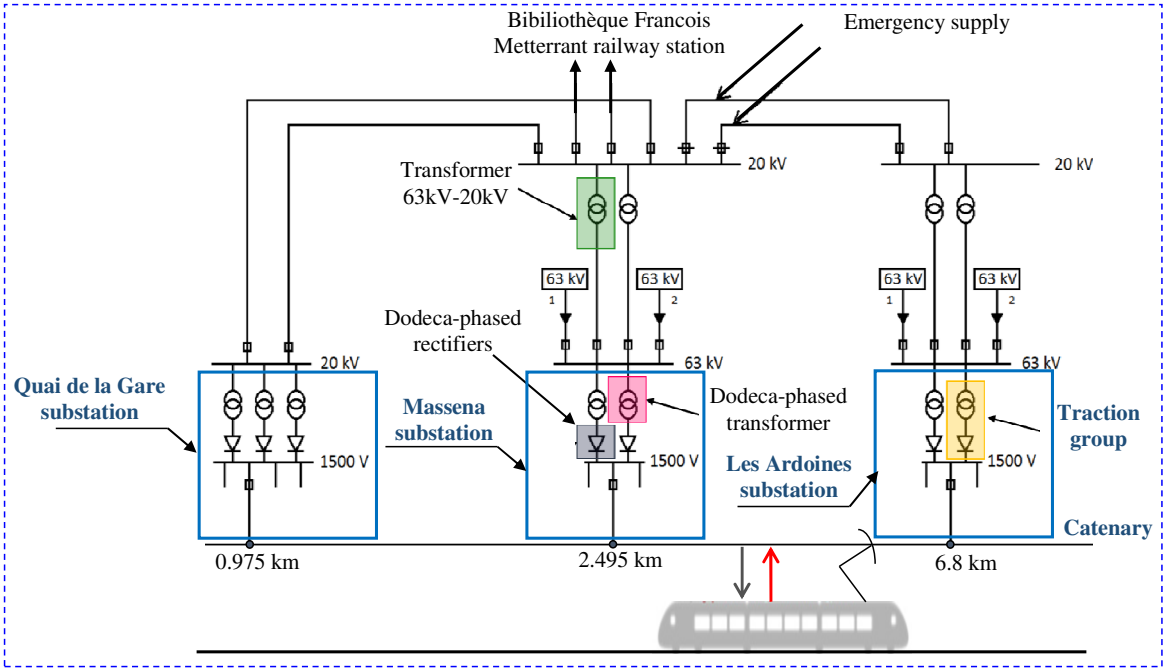

Fig. 1. The studied electrical railway network

3. Modeling of the railway electrical network

This section describes the different stages of modeling of the railway electric network studied in the "Masséna" project (Fig. 2). The railway power network consists of four main elements: substations, rails, catenary and trains.

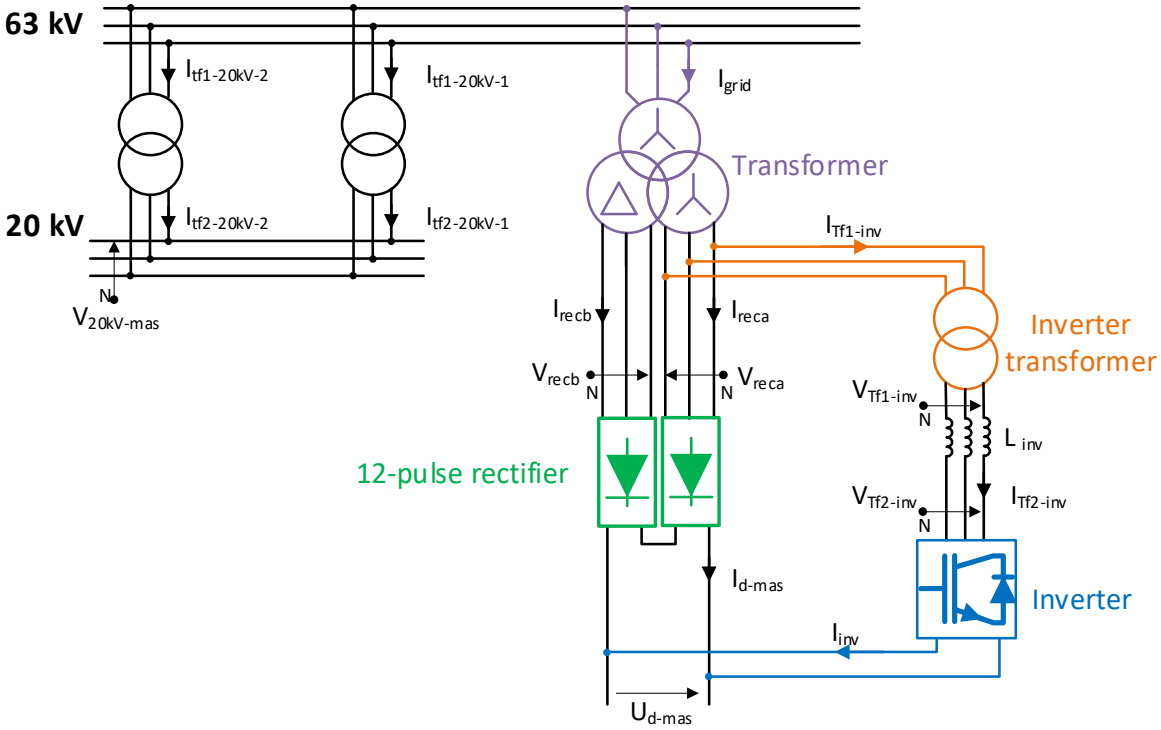

Fig. 2. The "Masséna" traction units (in green and magenta) and the additional inverter (in blue) structural descriptions

3.1. *Railway power system modeling*

The substations are the interface between the catenary and the AC electrical network. Thus, it is necessary to set up a model, which takes into account the AC and DC part of the railway power system. The "Masséna" substation contains two parallel 63 kV / 20 kV transformers, which supply "Quai de la Gare" substation and provide an emergency supply to "Les Ardoines" substation. Two other secondary double winding transformers supply two twelve-pulse rectifiers. Masséna transformers are considered ideal (iron and copper losses are neglected) and modelled by using an equivalent single-phase Thevenin model (Fig. 3). The modeling is adopted for the other two substations since all substations have the same type of traction unit. The twelve-pulse rectifier is made up of two three-phase rectifiers connected in series; a double parallel rectifier and a serial rectifier. The supply voltage systems of the two three-phase converters are assumed perfectly balanced.

As illustrated in Fig. 3, the twelve-pulse rectifier is represented by two DC voltage sources U_{d0a} and U_{d0b} in series with an equivalent resistor $R_{rec-mas}$ and a diode. Both DC voltage sources model the no-load voltage $U_{d\text{-}mas}$, which can be calculated from the AC rated voltages V_{reca} and V_{recb} of the transmission system [28].

$$\begin{cases} \langle U_{d-mas}(t)\rangle = \langle U_{d0a-mas}(t)\rangle + \langle U_{d0b-mas}(t)\rangle \\ U_{d0a-mas}(t) = \dfrac{3\sqrt{6}}{\pi} V_{reca}(t) \\ U_{d0b-mas}(t) = \dfrac{3\sqrt{2}}{\pi} V_{recb}(t) \end{cases} \quad (1)$$

The resistor $R_{rec\text{-}mas} = R_{reca\text{-}mas} + R_{recb\text{-}mas}$ models the DC voltage drops $\Delta U_{da\text{-}mas}$ and $\Delta U_{db\text{-}mas}$ that mainly come from the commutation overlap.

$$\begin{cases} \Delta U_{da-mas}(t) = \dfrac{3\sqrt{6}}{2\pi} V_{reca}(t)\left(1-\cos\left(\mu_{reca-mas}(t)\right)\right) \\ \Delta U_{db-mas}(t) = \dfrac{3\sqrt{2}}{2\pi} V_{recb}(t)\left(1-\cos\left(\mu_{recb-mas}(t)\right)\right) \end{cases} \quad (2)$$

where $\mu_{reca\text{-}mas}$ and $\mu_{recb\text{-}mas}$ are the encroachment angles. This phenomenon is due to the inductances $L_{a\text{-}eq\text{-}mas}$, $L_{b\text{-}eq\text{-}mas}$ (ie. transformer inductances) within the electrical circuit. In fact, the current within diodes does not turn off and turn on instantaneously.

$$\begin{cases} R_{reca-mas} = 3L_{a-eq-mas}\dfrac{\omega}{\pi} \\ R_{recb-mas} = L_{b-eq-mas}\dfrac{\omega}{\pi} \end{cases} \quad (3)$$

The encroachment time is equal to $\mu_{reca\text{-}mas}/\omega$ for the double parallel rectifier and to $\mu_{recb\text{-}mas}/\omega$ for the serial rectifier, with ω, the network natural frequency.

$$\begin{cases} \cos\left(\mu_{reca-mas}(t)\right) = 1 - \dfrac{\left(2\omega I_{d-mas}(t) L_{a-eq-mas}\right)}{\sqrt{6} V_{reca}(t)} \\ \cos\left(\mu_{recb-mas}(t)\right) = 1 - \dfrac{\left(2\omega I_{d-mas}(t) L_{b-eq-mas}\right)}{3\sqrt{2} V_{recb}(t)} \end{cases} \quad (4)$$

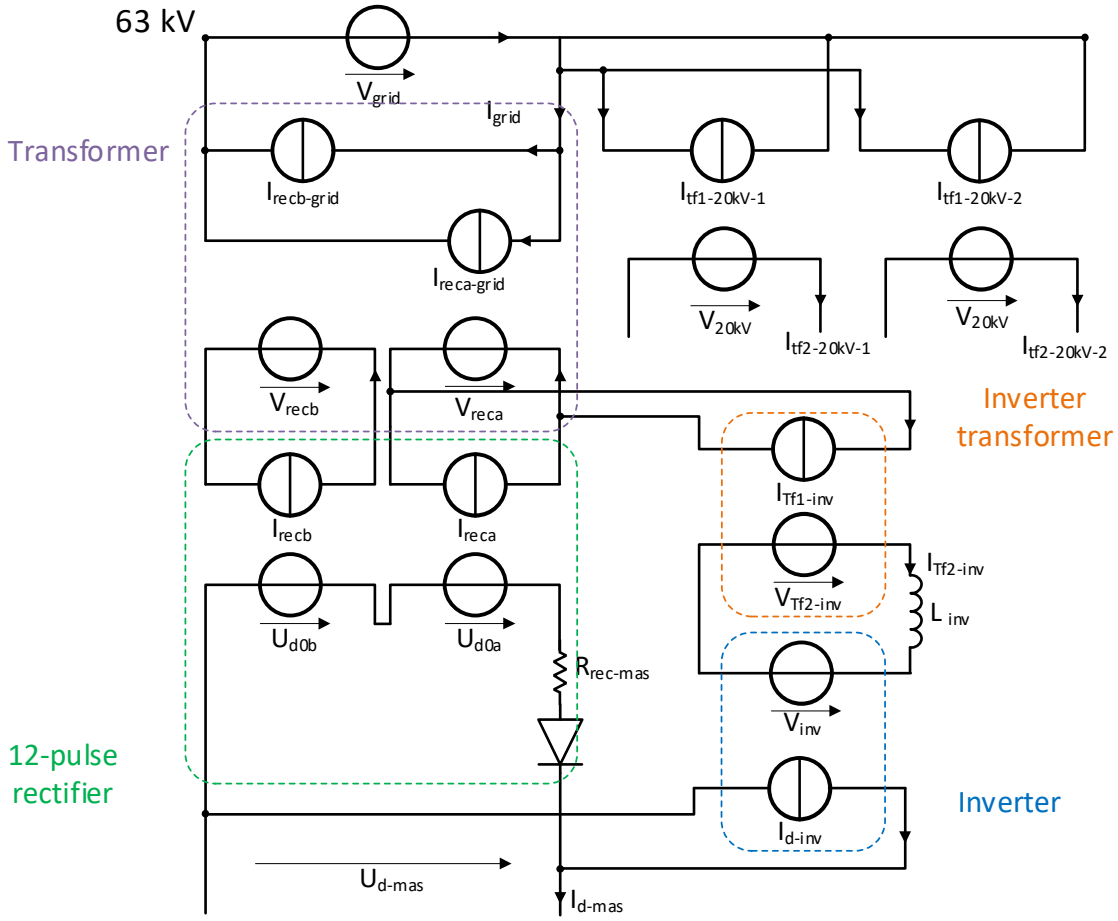

Fig. 3. Single-phase equivalent electrical circuit

As depicted in Fig. 3, the primary windings of the transformer are represented by reversible instantaneous AC current sources: $I_{reca\text{-}grid}$ and $I_{recb\text{-}grid}$, for the secondary double-wound transformer, $I_{tf1\text{-}20kV\text{-}1}$ and $I_{tf1\text{-}20kV\text{-}2}$ for the transformers for the adaptation from 63kV to 20kV. The primary currents are calculated as function of the secondary currents, I_{reca}, I_{recb}, $I_{tf2\text{-}20kV\text{-}1}$, $I_{tf2\text{-}20kV\text{-}2}$, using the transformers ratios, $k_{tf\text{-}Yy}$, $k_{tf\text{-}Yd}$, $k_{tf2\text{-}20kV\text{-}1}$, $k_{tf2\text{-}20kV\text{-}2}$.

$$\begin{cases} I_{reca-grid}(t) = k_{tf-Yy} \times I_{reca}(t) \\ I_{recb-grid}(t) = k_{tf-Yd} \times I_{recb}(t) \end{cases} \Rightarrow I_{grid}(t) = I_{reca-grid}(t) + I_{reca-grid}(t)$$

$$\begin{cases} I_{tf1-20kV-1}(t) = k_{tf2-20kV-1} \times I_{tf2-20kV-1}(t) \\ I_{tf1-20kV-2}(t) = k_{tf2-20kV-2} \times I_{tf2-20kV-2}(t) \end{cases} \Rightarrow I_{tf-20kV}(t) = I_{tf1-20kV-1}(t) + I_{tf1-20kV-2}(t) \quad (5)$$

The secondary windings are modeled by AC voltage sources V_{reca}, V_{recb} and V_{20kV}, which are obtained from multiplying the transformer ratio by the national grid voltage V_{grid} as following:

$$\begin{aligned} V_{reca}(t) &= k_{tf-Yy} \times V_{grid}(t) \\ V_{recb}(t) &= k_{tf-Yd} \times V_{grid}(t) \\ V_{20kV}(t) &= k_{tf2-20kV-2} \times V_{grid}(t) \\ V_{20kV}(t) &= k_{tf2-20kV-2} \times V_{grid}(t) \end{aligned} \quad (6)$$

Assuming that losses are negligible, the power balancing gives approximatively the RMS value of the fundamental component $I_{reca\text{-}RMS}$ and $I_{recb\text{-}RMS}$ of these currents and their phase shifts Φ_{reca} and Φ_{recb} which depend on the commutation overlap angles μ_{reca} and μ_{recb} [28].

$$I_{reca-RMS} \approx \frac{\sqrt{6}}{\pi} I_{d-mas}; \cos(\phi_{reca}) \approx \frac{(1+\cos(\mu_{reca}))}{2}$$
$$I_{recb-RMS} \approx \frac{\sqrt{2}}{\pi} I_{d-mas}; \cos(\phi_{recb}) \approx \frac{(1+\cos(\mu_{recb}))}{2} \quad (7)$$

3.2. *Modeling of trains*

Trains consist of four cars, two motorized cars and two passengers cars. Each motorized car has four 375 kW induction motors. Therefore, the total power involved in a double multiple unit train can be 6000 kW. Current source inverters supply the traction motors through a LC filter. They are modelled as a current source in parallel with a capacitor. In the simulation model, the train is considered as a reversible current source in parallel with a capacity, as depicted in Fig. 4. The capacitor value is calculated form the sum of capacitors of LC filters of all inverters supplying the train induction motors. The values of LC filter components are obtained from the train inverters datasheet.

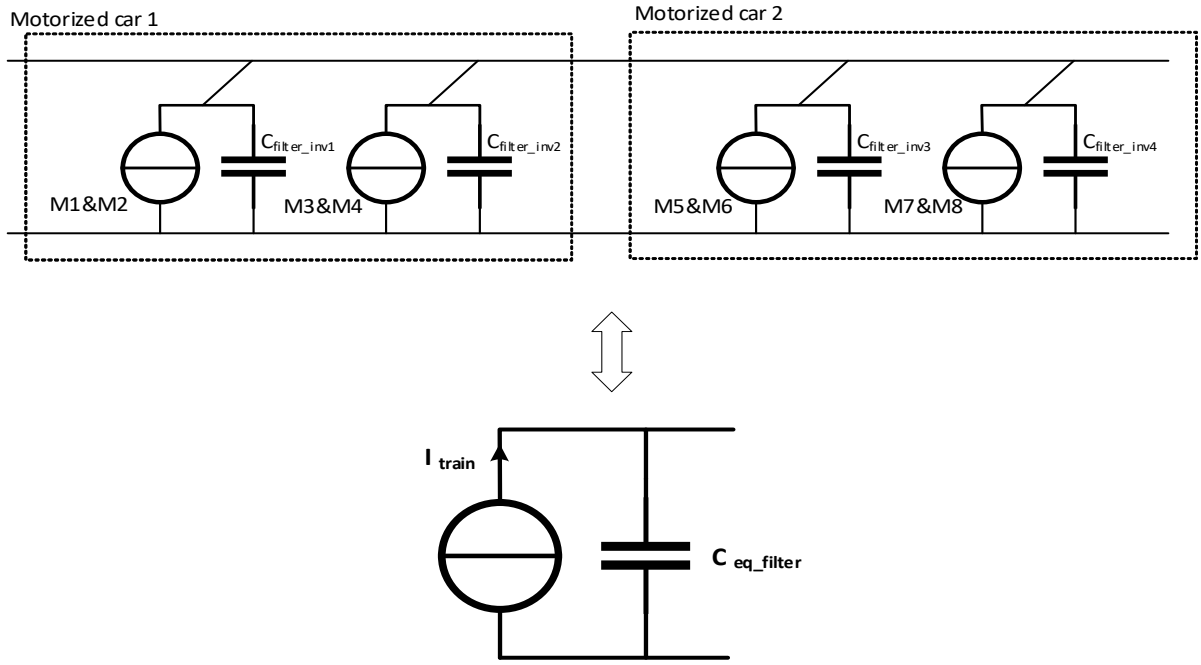

Fig. 4. Single unit train equivalent electrical model with catenary/rail resistances

As depicted in Fig. 5, there are four steps to calculate the traction/braking current as function of train data.

The resistive force $F_{res}(t)$ applied to the advancement of the train is obtained from the coefficients of the train speed V_{train} and the advancement resistance parameters k_0, k_1 and k_2:

$$F_{res}(t) = k_0 + k_1 \times V_{train}(t) + k_2 \times V_{train}{}^2(t) \quad (8)$$

Then, the total resistive force $F_{tot}(t)$ applied at the axles of the train is expressed as follows:

$$F_{tot}(t) = M_{train} \times Acc_{train}(t) + F_{res}(t) + M_{train} \times g \times \sin(\alpha) \quad (9)$$

where $Acc_{train}(t)$ is the train acceleration, M_{train} is the train mass, g is the coefficient of gravity, and α is the slope of the track.

These values are used to estimate the mechanical power produced at the train axles:

$$P_{mec}(t) = F_{tot}(t) \times V_{train}(t) \quad (10)$$

During traction, P_{elec} is obtained from the mechanical power P_{mec} at the axles, consequence of the acceleration and speed of train. Thanks to regenerative braking, some electrical power can be sent back to the catenary. This electrical power is deduced from P_{mec}, which, in braking, is linked to the deceleration ($P_{mec\text{-braking}}$) and restrained by the speed through the maximum convertible mechanical power $P_{mec\text{-convertible}}$.

Traction mode:

$$P_{elec}(t) = P_{mec}(t)\eta^{k} + P_{aux}; k = -1 \quad (11)$$

η is the efficiency of the traction unit and P_{aux} is the auxiliary power.

Regenerative braking mode:

$$P_{mec} = \min\left(P_{mec-convertible}, P_{mec-braking}\right) \quad (12)$$

The electrical power sent to the catenary is restricted by the coefficient γ, which controls the rise of the DC voltage and keeps it below its maximum limit. Considering the consumption of the auxiliaries P_{aux} and the traction chain efficiency η, the electrical power could be calculated as following:

$$P_{elec} = \gamma \times P_{mec} \times \eta + P_{aux} \quad (13)$$

The current I_{train} is derived from the train electrical power $P_{elec\text{-}train}$ with the voltage measured across their terminals $U_{d\text{-}train}$,

$$I_{train} = P_{elec} / U_{d-train} \quad (14)$$

where the train voltage $U_{d\text{-}train}$ is measured at the terminals of the capacitor.

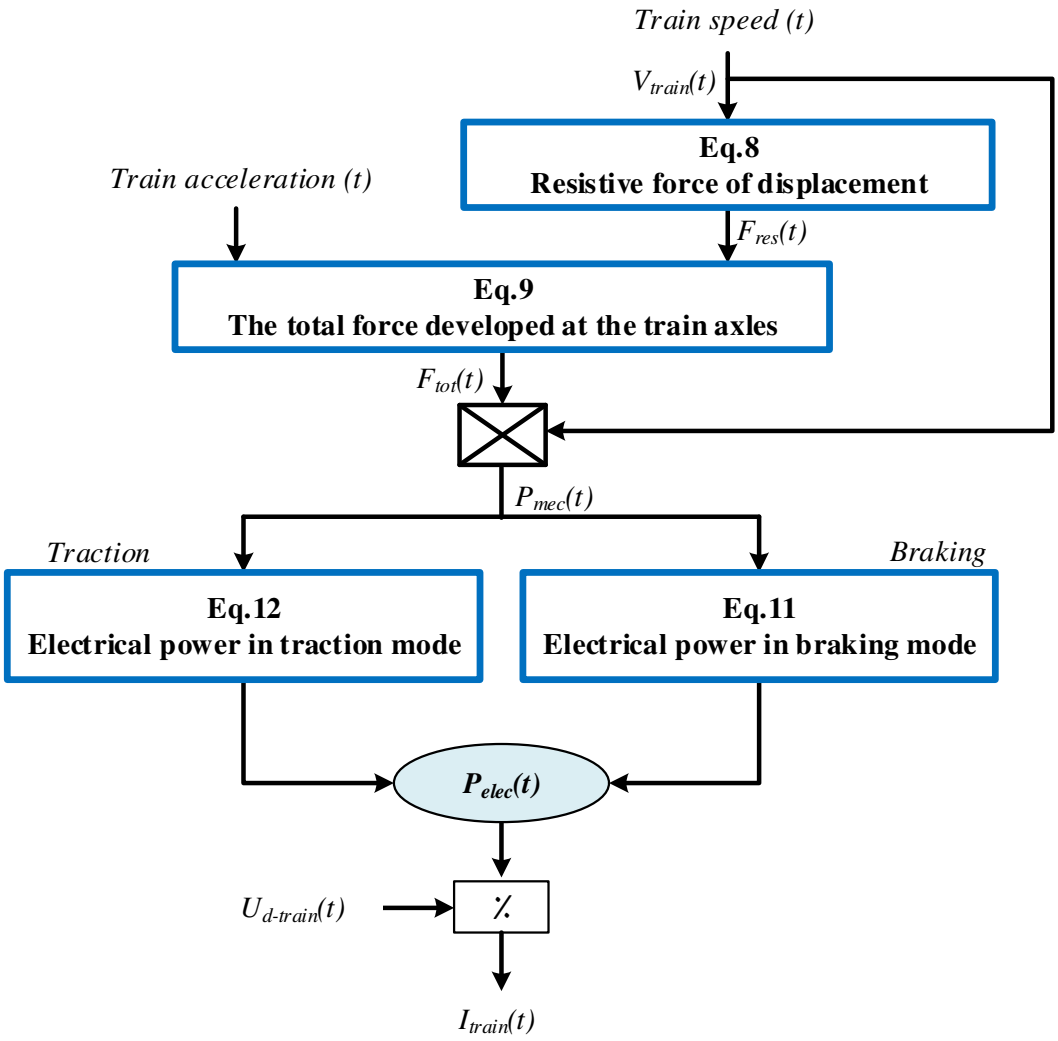

Fig. 5. Block diagram of the train modeling

3.3. *Modeling of train movement*

The running trains are fed through a catenary and the current is pathed via the rails. Therefore, the modeling of the traffic begins with the modeling of the rails and the catenary, which are considered as resistors and can be grouped under one resistance, as depicted in Fig 6.

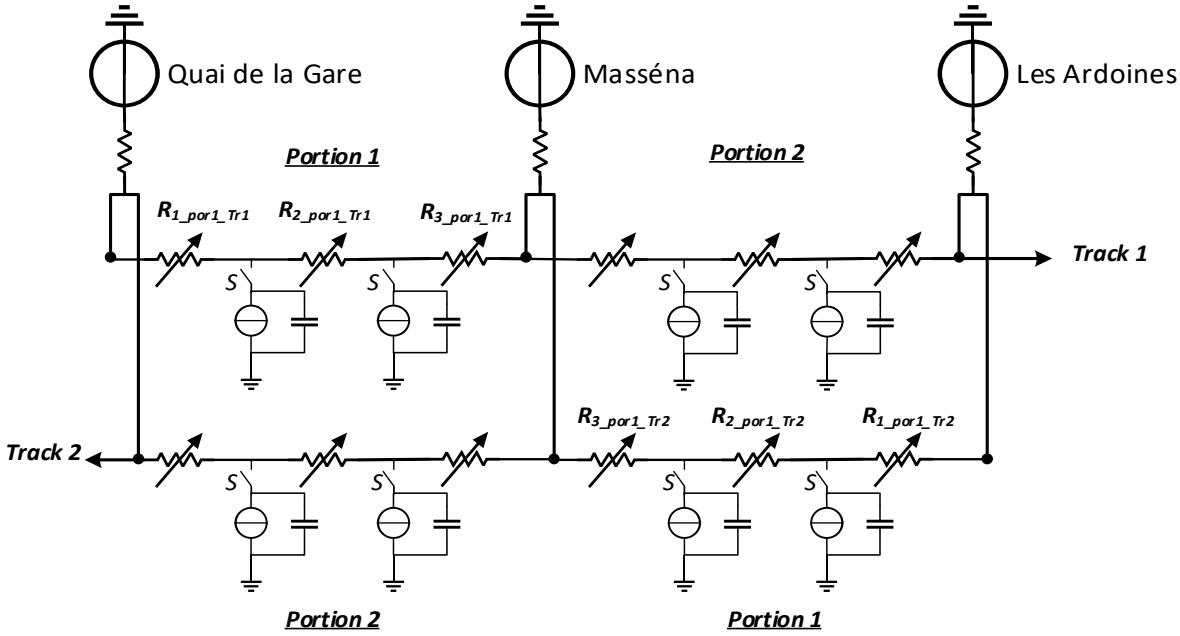

Fig. 6. Modeling of the complete line section

The studied line is made up of two tracks with opposite directions. For the direction "Quai de la Gare" towards "Les Ardoines". The route is divided into two portions:

- The first portion is between the "Quai de la Gare" and "Masséna" substations,
- The second portion is between the "Masséna" and "Les Ardoines" substations,

Each portion is likely to receive a maximum two trains. To model the train traffic on the entire track, each portion should be treated separately and could have three train-circulation cases:

- Two trains run on the track portion, the two modeled trains are connected and the rail and catenary resistances are calculated according to the distance between trains and the distance between trains and substations.
- One train runs on the track portion. One of the modeled trains is disconnected from the catenary by switch 'S'. For portion 1 of track 1, the values of $R_{1\_por1\_Tr1}$ and $R_{2\_por1\_Tr1}$ are calculated respectively as function of the distance between the train and the "Quai de la Gare" substation and the distance between the train and the "Masséna" substation, and $R_{3\_por1\_Tr1}$ is zero.
- No train run, so the two modeled trains are disconnected from the catenary. For portion 1 of track 1, $R_{1\_por1\_Tr1}$ is calculated according to the total length of the portion while $R_{2\_por1\_Tr1}$ and $R_{3\_por1\_Tr1}$ are zero.

The complete line is modeled by adding track 2. On track 2, the trains run in the opposite direction, i.e. from "Les Ardoines" to the "Quai de la Gare". To take into account the reversal of the direction in the calculation of the equivalent resistances of the catenary/ rail, we oriented the two tracks. Track 1 is with P_k positive while track 2 is with P_k negative. This calculation method has been implemented so that the equivalent catenary/rail resistance remains positive and increases in the direction of the train. To explain this point, considering this case study, two trains respectively at P_k = 1 km and at P_k = 5 km run on track 1 and on track 2. The calculation of the two resistances, $R_{1\_por1\_Tr1}$ and $R_{1\_por1\_Tr2}$ is done as follows:

$$\begin{cases} R_{1\_por1\_v1} = \left(position_{train} - position_{Quai\ de\ la\ gare} \right) \times R_{lineic\ catenary/rail\ resistance} \\ \qquad\qquad = \left(1 - 0.975\right) \times R_{lineic\ catenary/rail\ resistance} \\ R_{1\_por1\_v2} = \left(position_{train} - position_{Les\ ardoines} \right) \times R_{lineic\ catenary/rail\ resistance} \\ \qquad\qquad = \left(\left(-5\right) - \left(-6.8\right) \right) \times R_{lineic\ catenary/rail\ resistance} \end{cases} \tag{15}$$

In these two cases, the equivalent resistance remains positive and increases when the train moves away from the substation.

3.4. *Modeling and control of the installed inverter for the reversible substation*

The controller of the braking train must restrain the recovered power according to the catenary voltage. Therefore, when the traffic is low in the DC electrical circuit, the controller degrades the power injected following characteristics, which is defined by the manufacturer in order to respect the catenary voltage limit (Fig. 7a). On the other side, the inverter droop control prevents power flow from the AC side to the DC side. Thus, when the DC voltage of the inverter falls below a predefined threshold V_{conv_0}, the power reference of the inverter will be set to zero. While when the DC voltage of the inverter exceeds the threshold voltage V_{conv_0}=1810V, the reference power of the inverter will be modified according to the DC voltage as function of a predefined characteristic curve (Fig. 7b). Then, the current will be limited by both strategies, the regenerative braking control characteristic and the droop control characteristic [29].

Pure electric braking which can lead to recovery of almost all braking energy is the ideal operation to maximize energy efficiency in railway systems. However, this solution must guarantee that most of the recovered energy is consumed by other electrical charges. Otherwise, the train's electric brake controller must limit the recovered power as a function of the train DC voltage; it therefore dissipates part of the additional energy in braking resistors and can also promote pneumatic braking to respect the maximum limits of the catenary voltage and the safety adherence conditions. In this study, the train brake controller begins to limit the recovery rate when the voltage reaches 1780V (Fig. 7). When the voltage reaches the maximum limit "1950V", the brake controller stop any injection of power to the catenary [30].

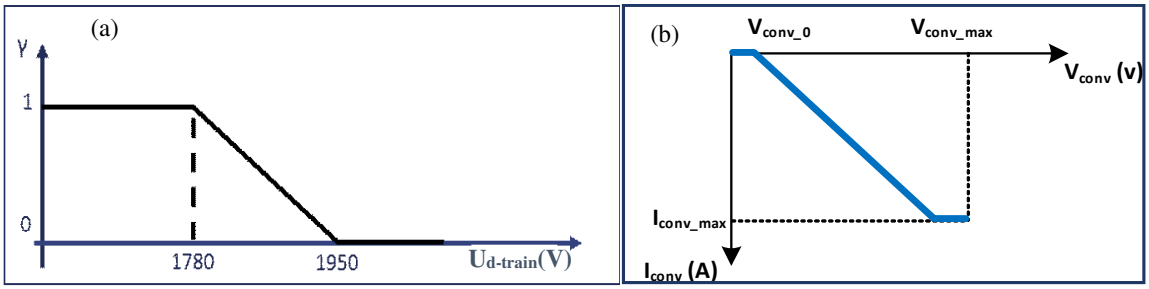

Fig. 7. (a) Coefficient for limiting the power produced by regenerative braking as function of the train voltage [27], (b) Characteristic of the inverter control

The modeling of the new inverter is based on single phase Thevenin sources. It is modelled by an equivalent DC current source, I_{dc} and an AC voltage source V_{inv} (Fig. 3). Its control consists of a voltage loop implementing a droop control (Fig. 8 and Fig. 9) and a current loop [28]. Those loops set the changeover voltage U_{dc_ref} between the rectifier and the inverter to 1810V. They regulate the active and reactive powers generated by the inverter. The droop parameter k is calculated as following:

$$k = -\frac{U_{d-mas-\max} - U_{dc\_ref}}{I_{inv-\max}} \tag{16}$$

where $I_{inv\text{-}max}$ is the inverter maximum current. The inverter sensibility to voltage deviation depends on the slope of the droop characteristic, which depends on the value of U_{dc_ref}. Given the droop parameters of the onsite actual 1 MW inverter, this maximum value is chosen to be V_{con_max}=1950 V.

With considering a maximum current of 1538A recommended by the inverter manufacturer, the droop parameter will be 0.091 Ω. The current reference of the current loop is given as following:

$$I_{d-ref} = \frac{U_{dc} - U_{dc\_ref}}{k} \tag{17}$$

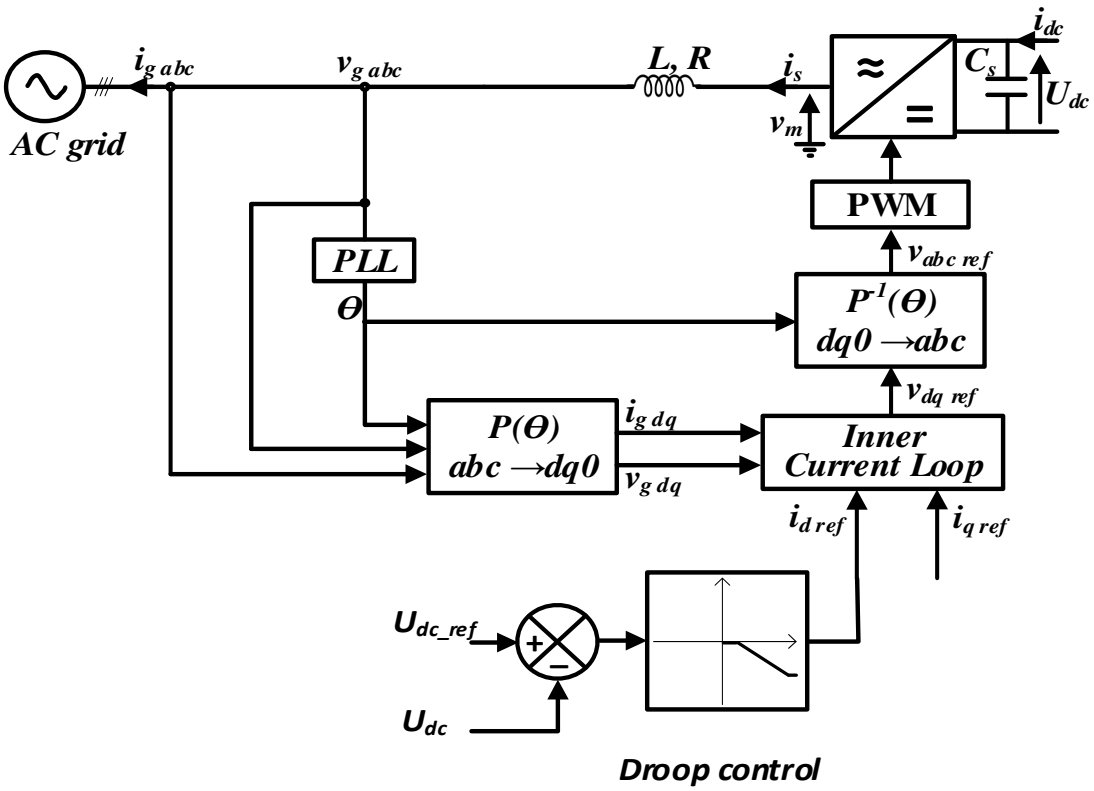

Fig. 8. Inverter control structure

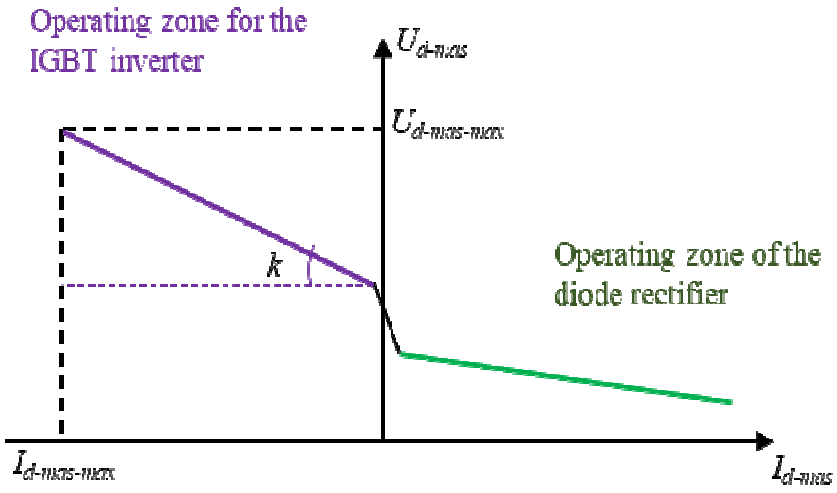

Fig. 9. Characteristic of the reversible "Masséna" power station

4. Implementation and simulation results

The model of the railway network and the SNCF rolling stock presented in section 3 is implemented in MATLAB / using functional blocks of Simscape for the train, substations, rails and catenary models. The Masséna inverter is modelled using Sim power system toolbox. The traffic input data of the simulation gives information about circulated trains such as, speed, position, acceleration for each step time. These input data are pretreated using MATLAB script in order to sort trains data by track and portion.

A traditional train speed profile is used for all cases presented in this section. It starts with an acceleration traction phase. The train pulls at a certain acceleration until it reaches the speed limit (120 km/h). Once the speed limit is reached, it goes into maintain constant traction phase (cruising phase),

which allows it to maintain this speed for a certain period. The next step is the coasting phase, which fixes at zero the traction force. Finally, the braking phase, such as the train brakes with a generally constant deceleration until its complete stop.
The simulation results of the proposed model are presented in the next three subsections. In the first subsection, two cases are considered; the first case aims to validate the studied model results, without Masséna inverter, with the ones obtained by the actual professional software Esmeralda. This software is used by SNCF in the conception phase of the railway system in order to choose the best location and power size of new substations and other infrastructure hardware. It assesses the technical and economical performances of the railway power network and evaluates the load demand for the national transmission grid. Esmeralda can be applied to many models of electrical infrastructure and rolling stock. This simulation considers the railway traffic, the electrical features of the trains and the architecture of power network as input data.
Since a main difference between the proposed modelling and Esmeralda modelling is the model of the inverter, a comparison between results of simulation with an inverter model added to Masséna substation is presented in a second case.
In the second subsection, results obtained using real-time simulation and laboratory inverter are compared to the results obtained with offline simulation. In such case, the control of the inverter is validated with a real low power scaled inverter and the dynamic of the proposed model are tested under real-time operation conditions.
The energetic efficiency of the railway system, concerned by this study, is investigated in the third subsection using the proposed simulation tool in order to evaluate the advantage of the installed inverter in Masséna substation to recover braking energy.

4.1. *Comparison with the professional railway software Esmeralda*

Since Esmeralda it is a professional software and plays an important role and its results have been compared and validated with experiments tests, it can therefore serve as a basis for validating the model presented in this study. This validation will be performed on simulations with the recovery inverter.
The same traffic scenario is adopted for both study cases in which the simulation results from Esmeralda and MATLAB are compared. In this scenario, the line portion taken in consideration is located between P_k=0 km and P_k=7 km. The traffic consists of two trains running in opposite direction on separate tracks. Fig. 10 presents the speed of each train for the proposed model and Esmeralda software. The first train starts its trajectory at t=0 s from "Quai de la Gare" to "Les Ardoines" and the second train starts its trajectory at=150 s from "Les Ardoines" to "Quai de la Gare". As depicted in Fig. 10, the slope can be considered as zero on this line, which knows very little difference in level. The power consumption of the railway station “Bibliothèque François Mitterrand” is neglected. The trains are following the same driving sequence but with a different kinematic.

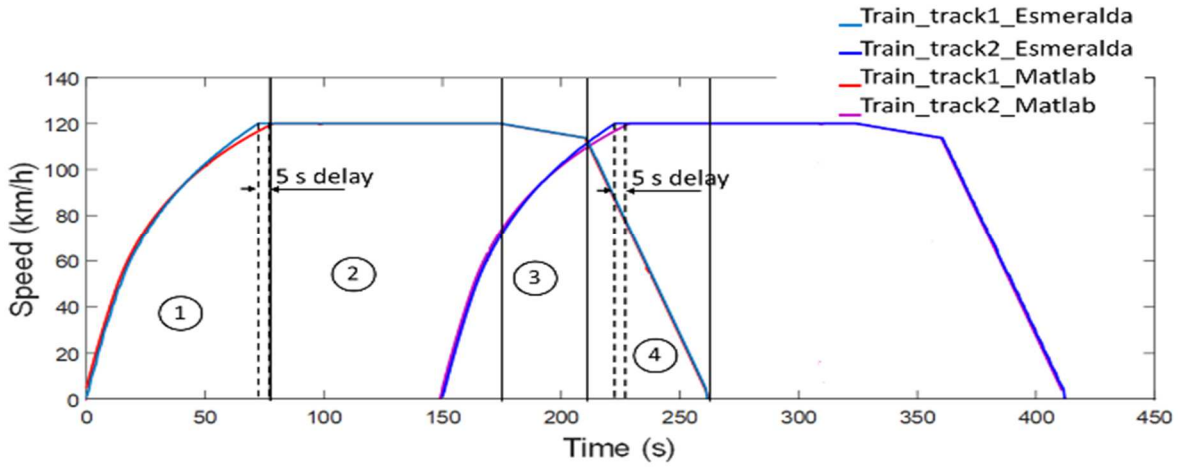

Fig. 10. The trains speed for the case study. (Acceleration (1), constant speed (2), coasting (3) and braking (4))

At the end of the acceleration phase, trains speeds in Esmeralda simulation are 5 s in advance in comparison with the ones obtained by MATLAB. This difference has a very limited effect on the train position (Fig. 11) and is due to the computational steps. Indeed, the Esmeralda's time step is derived from a fixed spatial data and is consequently variable, whereas the step time size used for MATLAB simulations is fixed. As the goal is to perform a validation of the model presented in this paper, voltages and powers of trains and substations without inverter are compared.

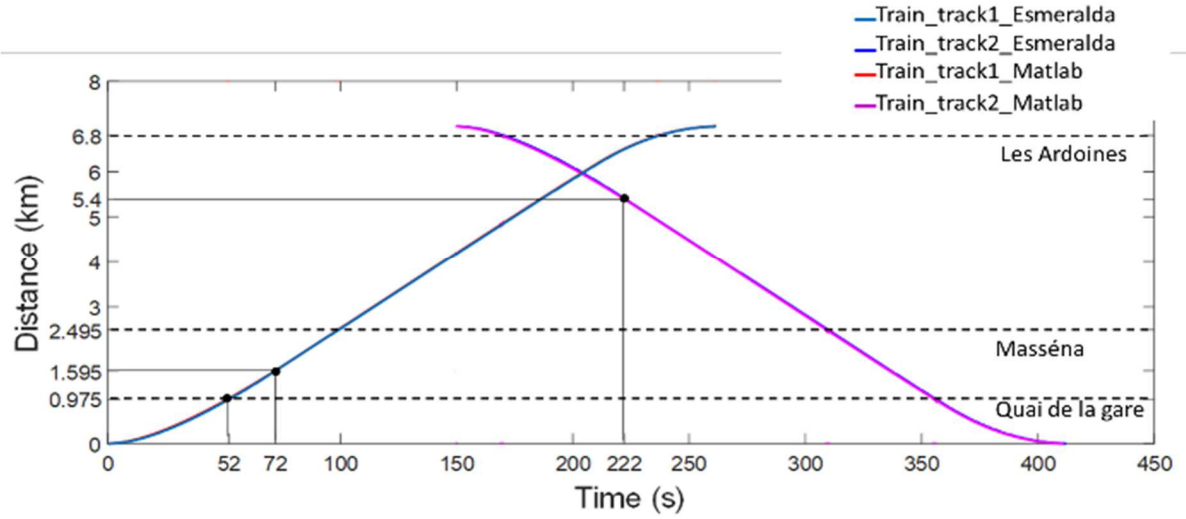

Fig. 11. The trains and substation position

First, the trains' power is addressed. In Fig. 12, the speed difference during acceleration found in Fig. 10 induces a 5 s delay in the train power. The braking sequences indicate also a braking lag. The electrical braking in Esmeralda is not instantaneous. It takes 3 s before being effective. This lag models the first pneumatic braking reaction, which is not taken into account in the model on MATLAB. The delays and time lags reverberate automatically on the other power and voltage results (Fig. 13, Fig. 14, Fig. 15 and Fig. 16).

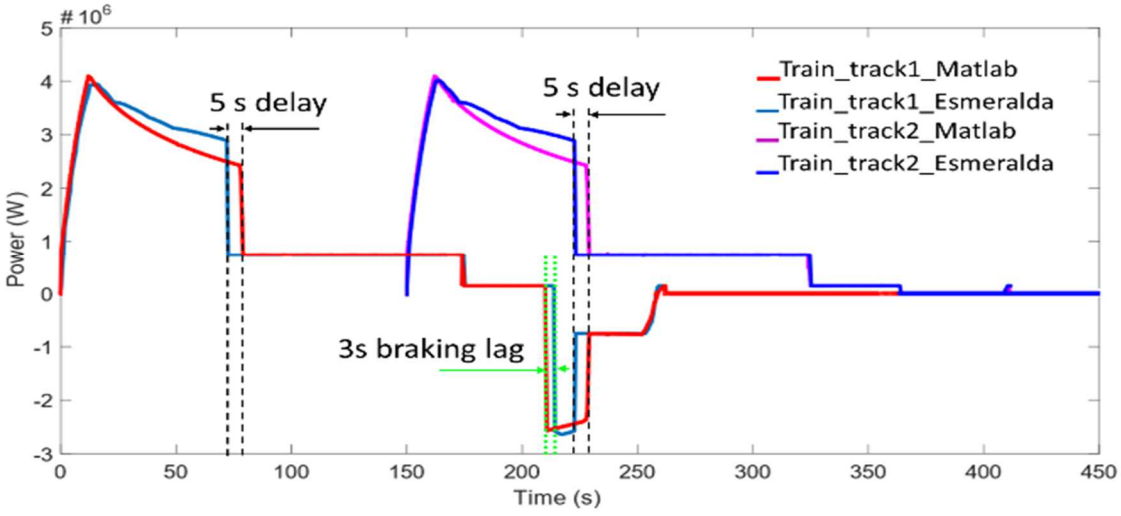

Fig. 12. The trains power without inverter vs time

The speed difference creates also a discrepancy on trains' power (see Fig. 12 and Table II). This new discrepancy influences substations results and trains' voltage in a less obvious manner that will be explained in the next paragraphs.

Table II. The voltage and power gaps for trains and "Masséna" substation

Maximum power gap for train 1	**400 kW (during acceleration sequence)**
Maximum power gap for train 2	400 kW (during acceleration sequence)
Train 1 maximum voltage gap	12 V (during acceleration sequence)
Train 2 maximum voltage	42 V (during acceleration sequence)
"Masséna" maximum power gap	245 kW
"Masséna" maximum voltage gap	190V

The voltage of train running on track 1 is investigated. Because Esmeralda train consumes more energy at the end of acceleration, its voltage remains lower than MATLAB (Table I and Fig. 13).

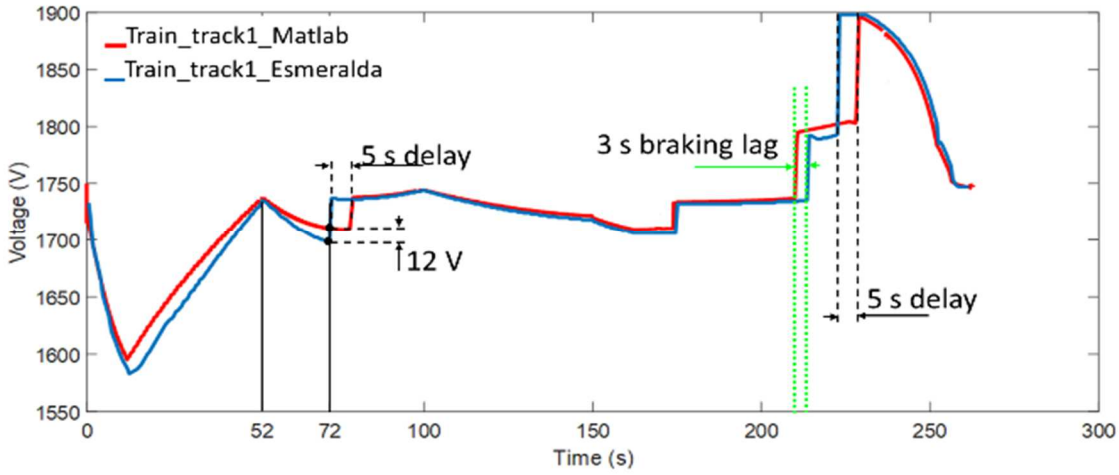

Fig. 13. The train voltage on track 1 without inverter

However, at 52s, the train on track 1 in both simulation Esmeralda and MATLAB are exactly located at "Quai de la Gare" substation (Fig. 11). Their voltages are then equal to the substation voltage (Fig. 13). Regarding trains on track 2, the biggest voltage difference is 42 V at 222s (Table II and Fig. 14). The power discrepancy effect is accentuated by the distance between the train on track 2 and substations, which are more important (Fig. 11). Consequently, the impedances and voltage losses rise.

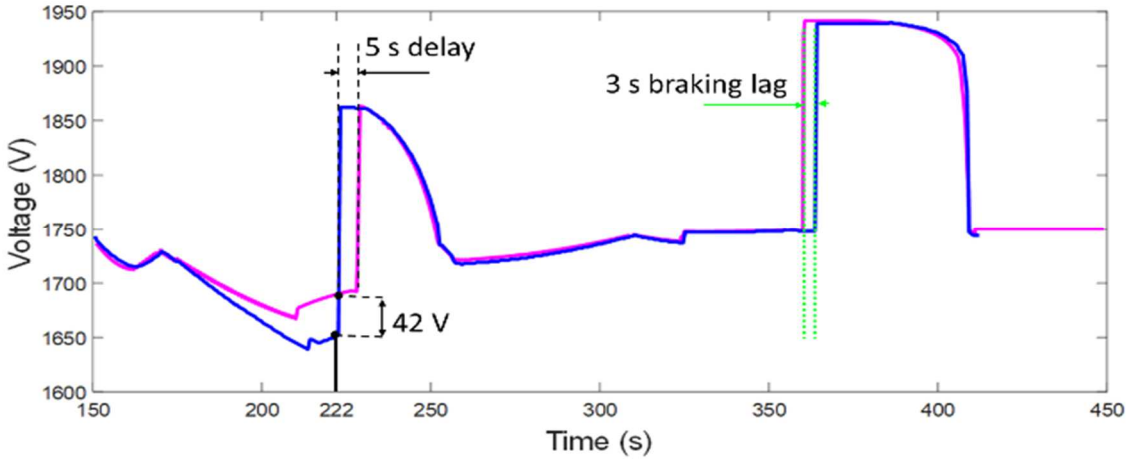

Fig. 14. The trains voltage on track 2 without inverter

Concerning "Masséna" substation, a 245 kW power gap is noticeable at 222s (Fig. 15).

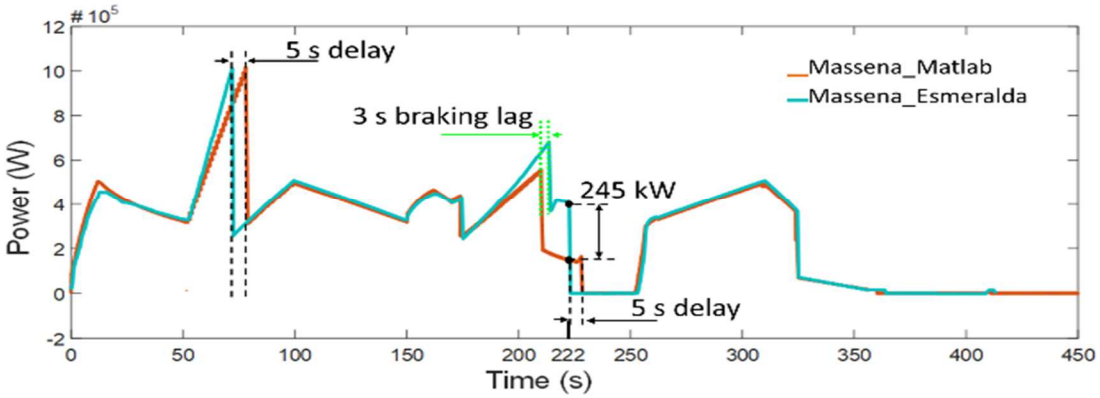

Fig. 15. The power of "Masséna" substation without inverter

Indeed, the braking train cannot supply all the energy demanded by the rolling train. "Masséna" by being near during this timeframe, can provide a part of the missing energy, which is more important in the simulation with Esmeralda. As presented in Fig. 16, the differences for the substation voltage are maximum during trains' braking sequences because these voltages are computed differently in Esmeralda and in Simulink. In Esmeralda model, the current delivered by the substations are used for deducing the voltage at their terminals. As, the currents are null during braking, the voltages of substations are equal to the no load voltage while, in the proposed model, the braking train sets the voltage in the power network by taking into account the power demanded at the catenary. The voltages of other trains and substations are then drawn from the braking train voltage.

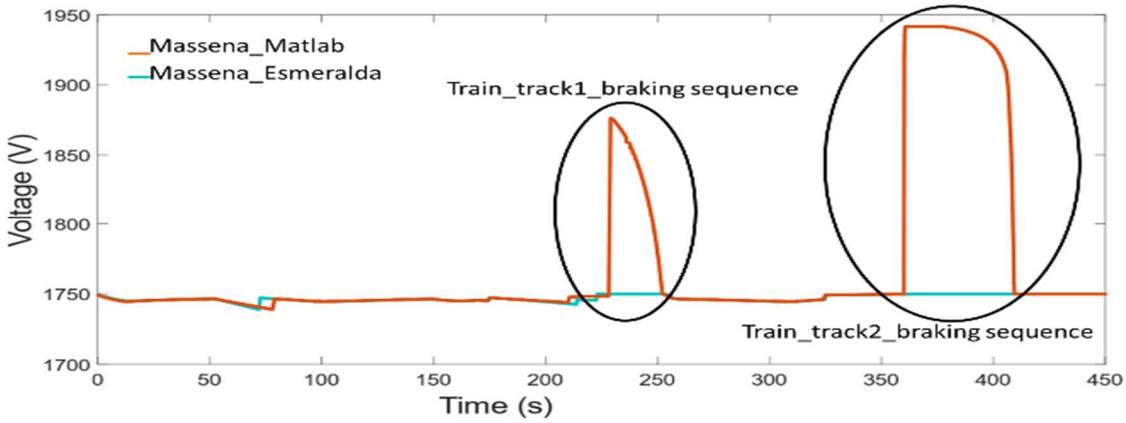

Fig. 16. The voltage of "Masséna" substation without inverter

Finally, the main differences between the results from the proposed model and Esmeralda model are explained by the gaps in input data. The comparison without inverter can be, then, a first validation of the proposed modeling.

As "Masséna" substation will be made reversible, SNCF has also made some simulations implementing the new inverter. Their goal was to estimate roughly, on Esmeralda, the energy that could be recovered. The inverter was modelled as a storage system able to receive energy when "Masséna" substation's voltage is higher than 1750V (the no load voltage). In Esmeralda, trains produced extra braking power which is completely recovered by the inverter (excepted for catenary losses) (Fig. 17). The recovered power reaches a 2 MW peak and the energy is estimated to 17 kWh. Because of the strategy implemented in Esmeralda, the inverter voltage is set and kept steady above the no load voltage during braking sequences (Fig. 18). The braking train voltage (Fig. 19) is calculated thanks to the inverter voltage. The braking power delivered is a consequence of the train's voltage obtained.

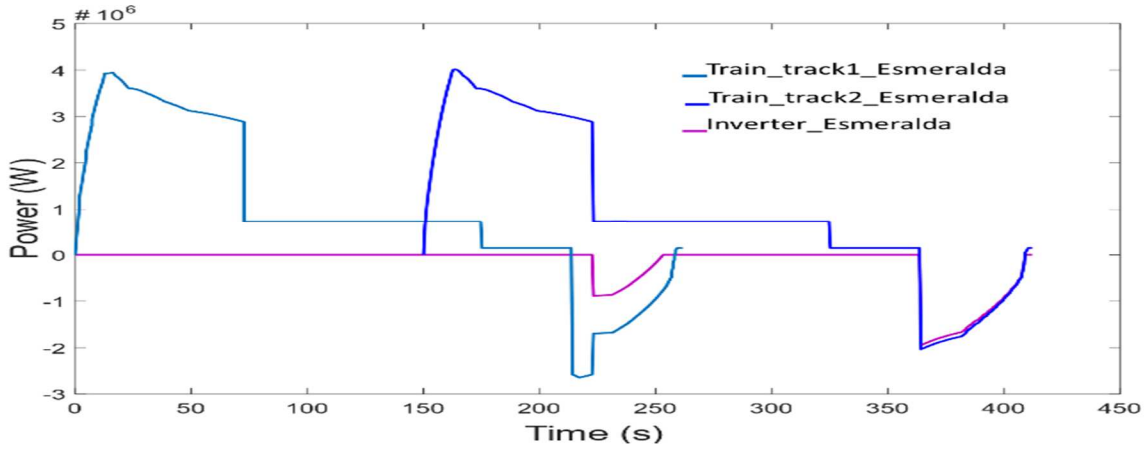

Fig. 17. The inverter and train power in Esmeralda

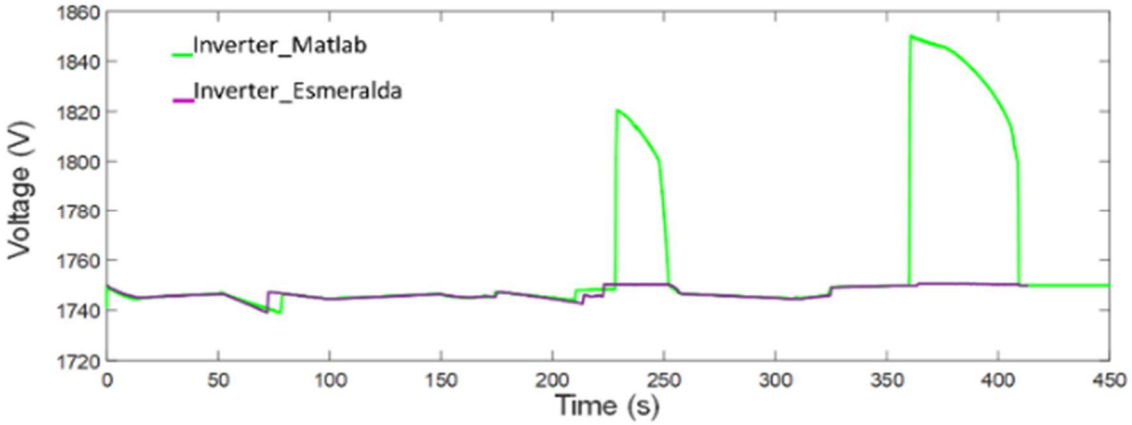

Fig.18. The voltage at the terminals of the inverter

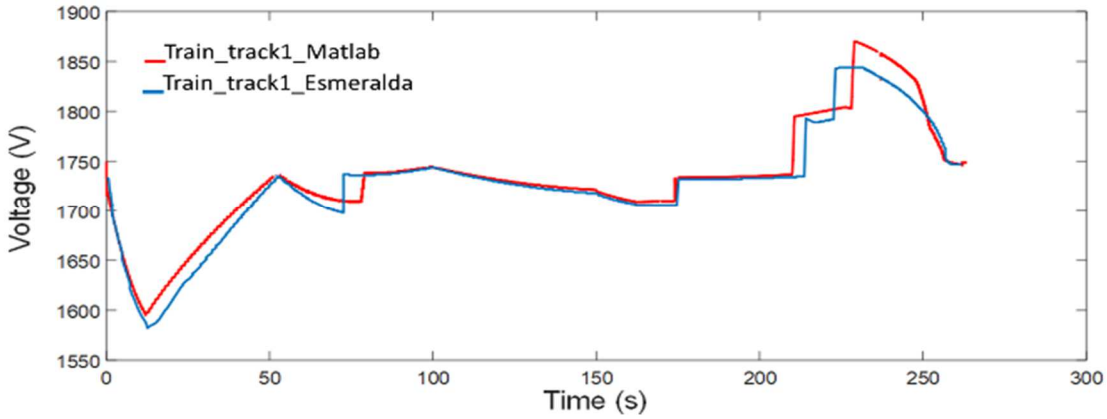

Fig. 19. The voltage at the terminals of the train running on track 1 with inverter

With the implemented model in MATLAB environment, the trains, also, produce braking energy which is pathed towards the inverter energy (Fig. 20). The extra braking energy is about 8.5 kWh with a 1 MW peak power. The recovered energy for the proposed model is less important with the simulation on Esmeralda because with the latter, the inverter was modelled as a storage system able to receive energy and the inverter voltage is set and kept steady above the no-load voltage during braking sequences. However, for the proposed model, an average model of an inverter with droop control is considered, so the voltage during braking sequences is variable and follows the inverter drop characteristics (Fig. 7). The recovered energy is twice smaller because with the real control strategy, the trains voltage in MATLAB are higher (Fig. 20), and the coefficient γ (13), which decreases with the voltage is then small.

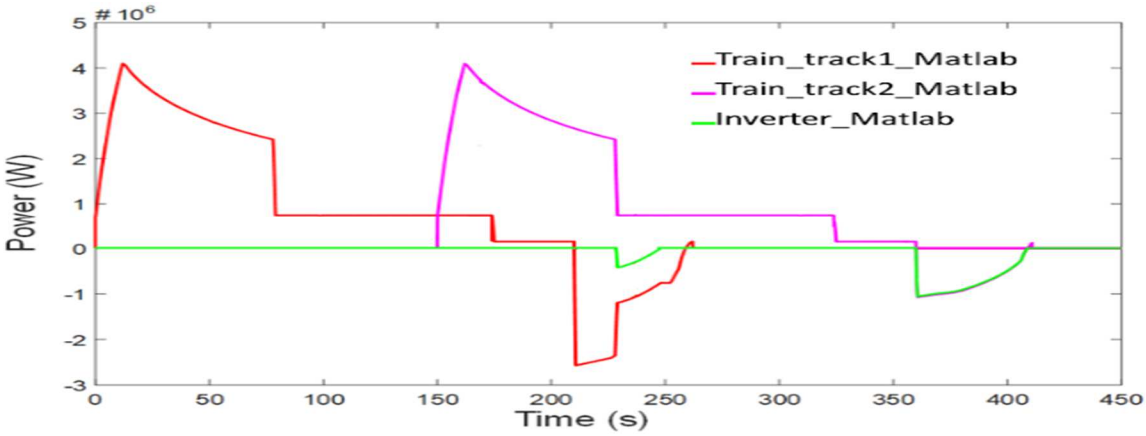

Fig. 20. The inverter and train power in MATLAB

4.2. *Experimental validation using Power-Hardware-In-the-Loop simulation*

For further validation of the proposed model, and since a direct implementation on the real railway system needs a long logistic and technical preparation, a PHIL simulation is used as a way to provide this kind of experimental results. The concept of PHIL consists of replacing the simulated hardware under test with a real hardware that interacts with an emulator, which reproduces the behavior of the remaining simulated model [31, 32]. Therefore, the behavior of the hardware can be investigated under appropriate conditions.

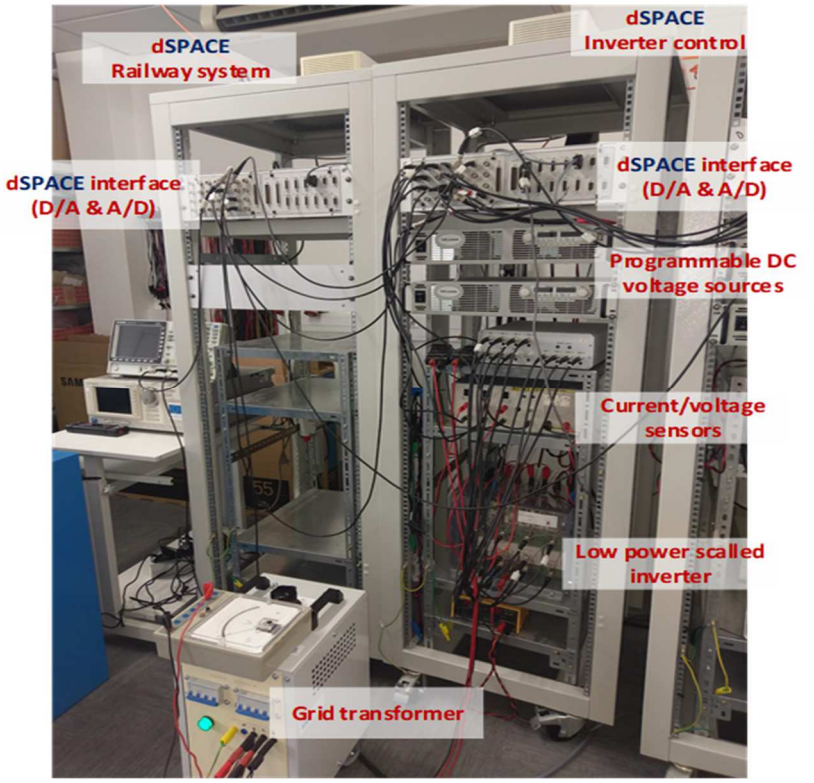

Fig. 21. Power-Hardware-In-the-Loop testbed

The connection between software and hardware parts is established via an interface in order to adapt voltage and power scale of the simulated part of the system to voltage and power scale of the real part (Fig. 21). For this study, the railway section presented in Fig. 1 is simulated in real-time by using a dSPACE 1103 platform with a sample time of 400 µs. The 1 MW reversible converter is replaced by a laboratory Semikron converter based on SKM50GB123D IGBT module. The nominal power of the used converter is considered to be 1 kW. The control is based on the same droop characteristic used

for the control of the onsite 1 MW inverter with considered gains of voltage and current. This converter is virtually connected to the simulated system by using a programmable DC voltage source TDK Lambda (GEN-600-5.5-3P400). The reference of the DC source is obtained from the DC voltage measurement of the simulated "Masséna" substation after being multiplied by a voltage adaptation gain $1/G_v$. The DC current measured in the real converter is sent back to the simulated system and multiplied by a current gain G_i then, it is injected in the modelled "Masséna" substation by using a controlled current source (Fig. 21 and Fig. 22) [31].

A real-time simulation of the proposed model in Section 4 needs a high-performance simulator. With the available dSPACE 1103 platform, some simplifications of the railway system model are considered to perform a real-time simulation (RTS) with an acceptable small sample time. The impacts of AC parts of the system are neglected and the substations are considered as ideal DC voltage sources. The considered railway section is shorter than the one presented before, it starts at 0.975 km ("Quai de la Gare" substation) and ends at 6.8 km ("Les Ardoines" substation).

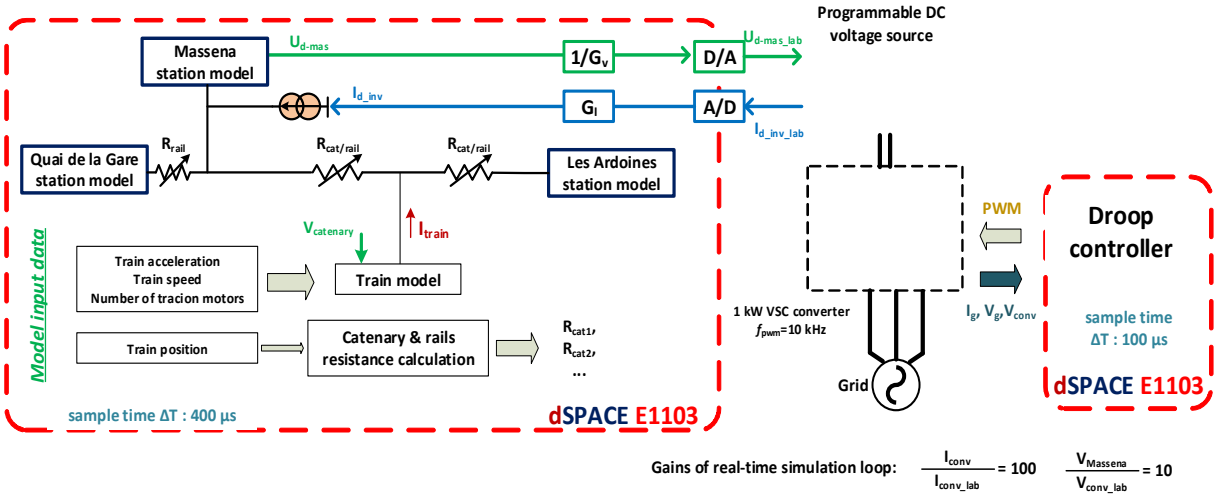

Fig.22. Representative diagram of the PHIL simulation used for the study

4.3. *Comparison between offline simulation and Real-time simulation*

For sake of simplicity, one train is running on the considered section of the railway system with a basic speed profile presented in Fig. 23. According to this profile, the train starts its trajectory in "Quai de la Gare" substation and stops at "Les Ardoines" substation.

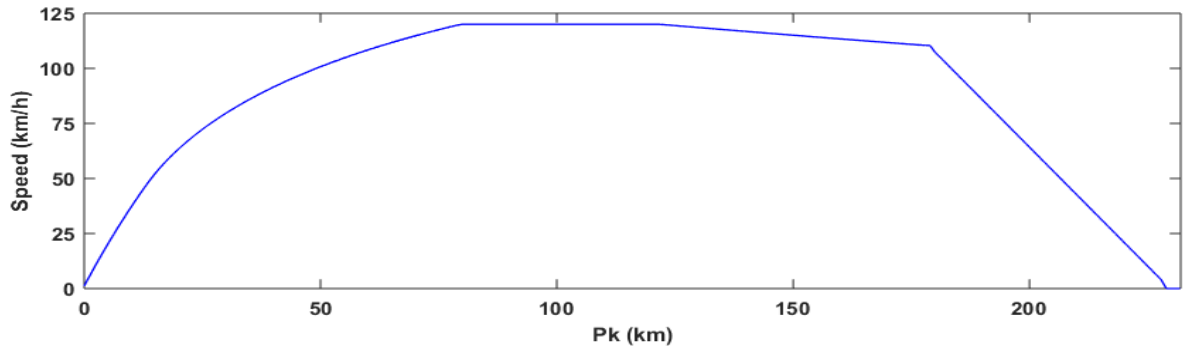

Fig. 23. Train Speed profile used for PHIL study

The train power measurement shows a good fit between MATLAB simulation and RTS simulation in traction phase. However, the recovered power during braking shows a difference of 143 kW (Fig. 24). This difference is originated from the DC voltage difference found on the train voltage and "Masséna" substation voltage measurements (Fig. 25, Fig. 26). This could be explained by the considered simplification for the railway system model used for the real-time simulation in terms of the length of the considered section and the substations.

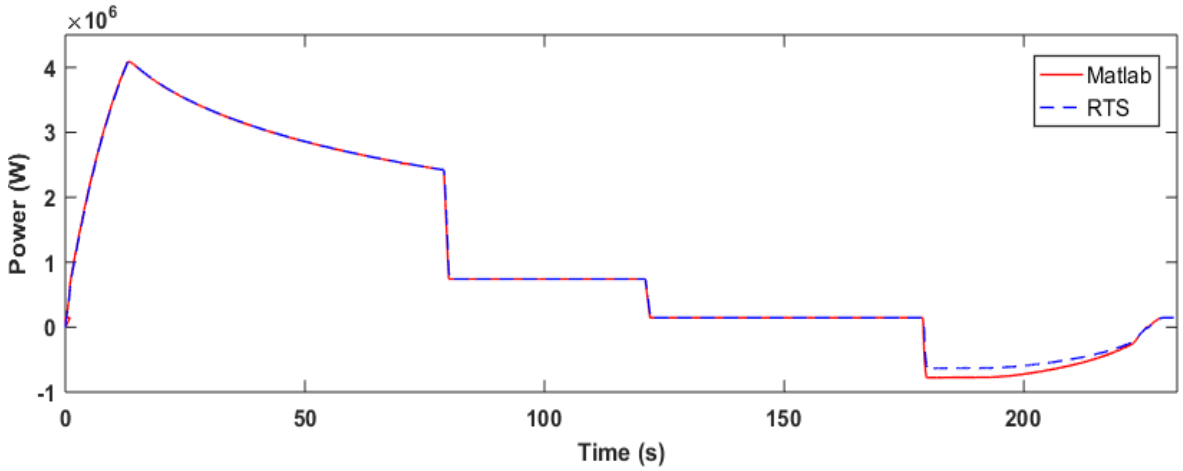

Fig. 24. Train power in offline simulation (MATLAB) and PHIL simulation (RTS)

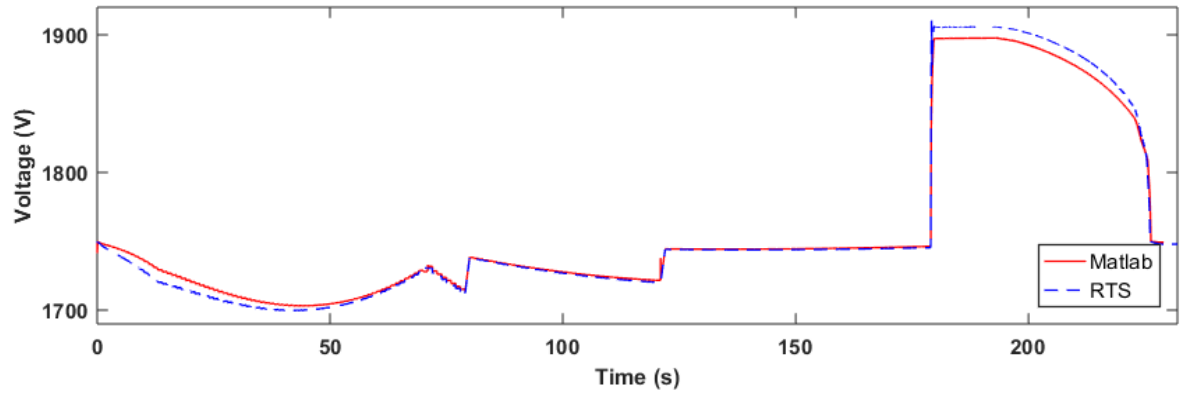

Fig. 25. Train voltage in offline simulation and PHIL simulation

The measurements of current and voltage of the laboratory 1 kW inverter are illustrated in Fig. 27. The DC voltage corresponds to the DC voltage of "Masséna" substation with a gain of 1/10. The ratio between the real current and the current injected in "Masséna" is 1/100.

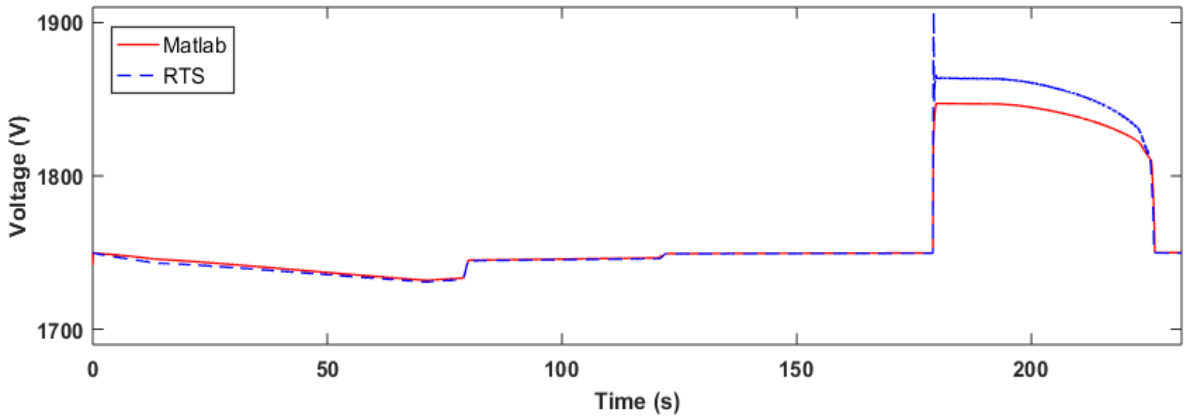

Fig. 26. "Masséna" substation voltage in offline simulation and PHIL simulation

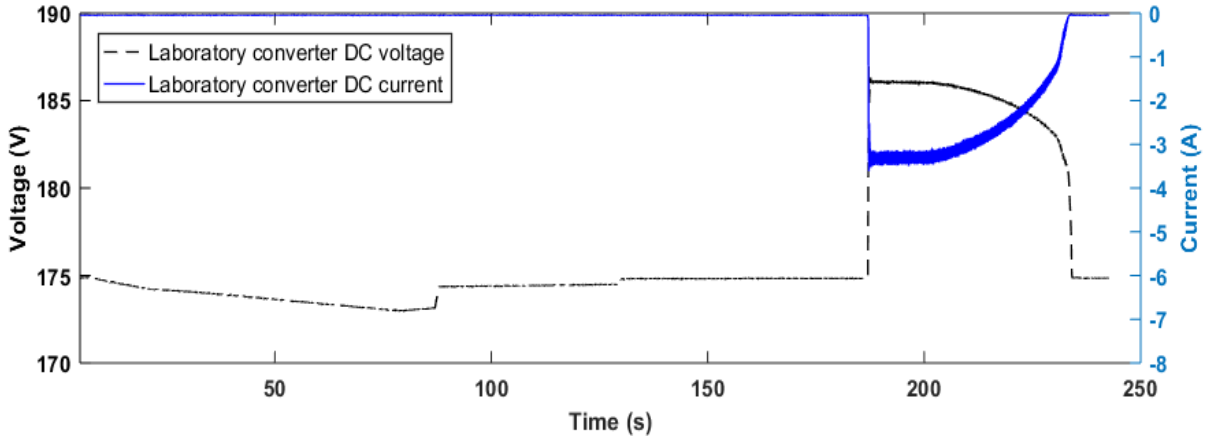

Fig. 27. Current and voltage of the laboratory 1kW converter

4.4. *Energetic efficiency study*

The main application of the proposed model is the estimation of the energetic saving due to the inverter installed in "Masséna" substation. In this section, a simulation of one hour of traffic (from 8am to 9am) is performed by using the model of the specific railway section. Input data of trains locations are illustrated in Fig. 28.

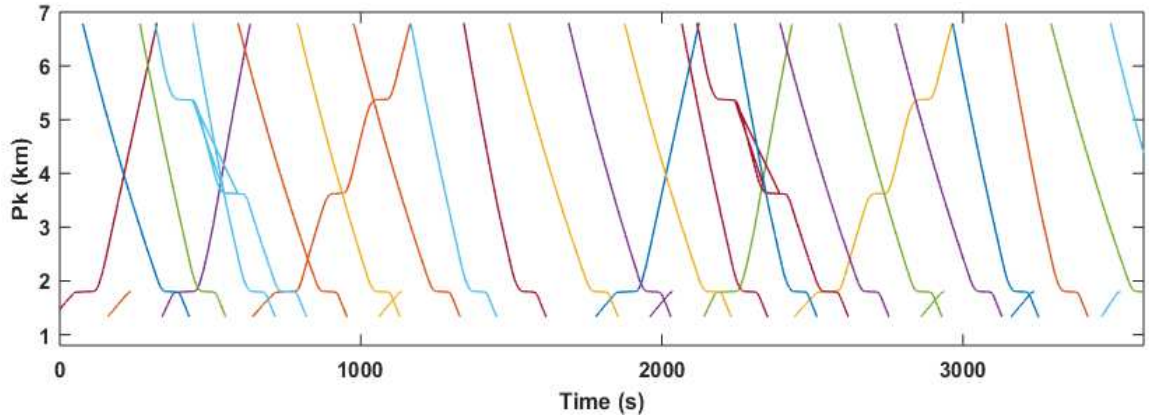

Fig. 28. Trains timeline for one-hour simulation

The power during traction phase and braking phase for each train circulating on the considered section is shown in Fig. 29. A part of the regenerative braking power provided by braking trains could be consumed by other trains in traction. The extra power is recovered by the inverter installed in "Masséna" (Fig. 30).

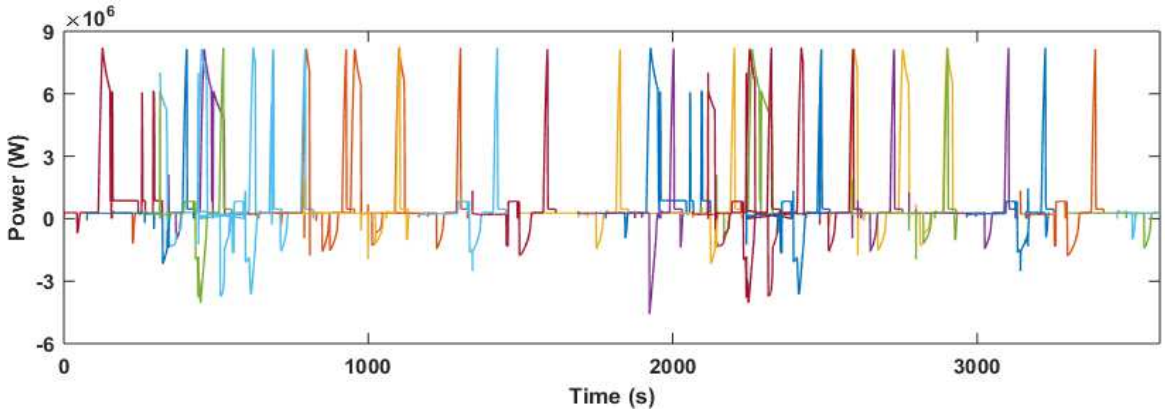

Fig. 29. Train power for one-hour simulation

As illustrated in Fig. 31, the total energy consumption of all trains is 2102 kWh. The major part of this energy is provided by the grid (2010.5 kWh) and the other part is provided by regenerative braking energy, which gives a total of 326.8 kWh. The extra energy is recovered by the inverter with a total of 139.4 kWh.

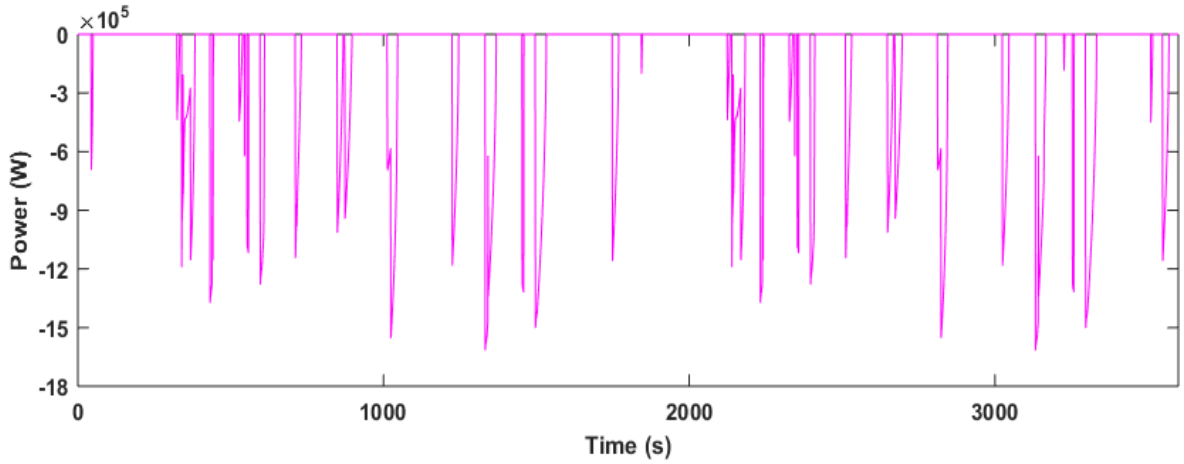

Fig. 30. Recovered power by "Masséna" inverter for one-hour simulation

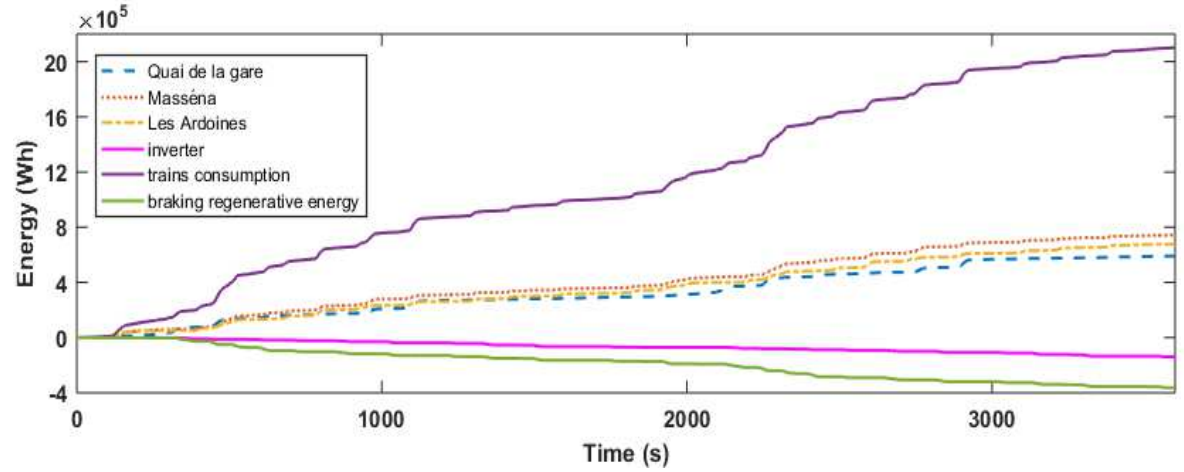

Fig. 31. Energy measurements for one-hour simulation

However, the energy balance, which could be calculated from Table II leads to deduce energy losses in the catenary and rails resistances with a total of 131 kWh.

Table II. Energy measurements for one-hour traffic simulation in (kWh)

Quai de la Gare	**Masséna**	**Les Ardoines**	**Trains consumption**	**Total regenerative energies**	**Inverter recovered energy**
591	742.4	677.1	2102	362.8	139.4

The energy restored and sent back to the grid by the inverter represent 6.934% of the total energy provided by the grid. This energy saving depends on several factors like the traffic density, inverter control and human factors like driving behaviors of train conductors.

5. Conclusion

This paper proposes a modeling of a DC power railway network including a power station, which was made reversible by adding a controllable inverter. The modeling is based on AC and DC equivalent

electrical sources for trains, reversible and non-reversible substations. The model without inverter is compared to the model, which is used by the professional SNCF software Esmeralda. This software, designed for sizing new substations, gives certified and reliable results. The comparison aforementioned allows to validate the model without inverter despite some gaps in voltage, power and current results. A second comparison with the inverter was also carried on. This comparison results in large differences in the power recovered with the inverter which, was twice smaller with the modeling presented in this paper. This is mainly due to the fact that the power electronic inverter and its control are taken into consideration in this modeling. The proposed model has been validated by using a PHIL simulation with an external laboratory scaled inverter and is then used to simulate one-hour traffic. The results show a gain of 6.9% in term of recovered energy by the inverter and so the energetic efficiency of the railway network is increased.

References

[1] W. Yuan, H. C. Frey, Potential for metro rail energy savings and emissions reduction via eco-driving, Applied Energy, 268, 2020, 114944.

[2] I. González–Franco, A. García–Álvarez, Can High–Speed Trains Run Faster and Reduce Energy Consumption? Procedia - Social and Behavioral Sciences 48 (2012) 827-837.

[3] A. Gonzalez-Gil, R. Palacin, P. Batty, Sustainable urban rail systems: Strategies and technologies for optimal management of regenerative braking energy, Energy Conversion and Management 75 (2013) 374–388.

[4] H. Liu, M. Zhou, X. Guo, Z. Zhang, B. Ning, T. Tang, Timetable Optimization for Regenerative Energy Utilization in Subway Systems, IEEE Transactions on Intelligent Transportation Systems 20(9) (2019) 3247–3257.

[5] X. Yang, B. Ning, X. Li, T. Tang, A Two-Objective Timetable Optimization Model in Subway Systems, IEEE Transactions on Intelligent Transportation Systems 15(5) (2014) 1913–1921.

[6] F. Hao, G. Zhang, J. Chen, Z. Liu, D. Xu, Y. Wang, Optimal Voltage Regulation and Power Sharing in Traction Power Systems with Reversible Converters, IEEE Transactions on Power Systems, (2020). 10.1109/TPWRS.2020.2968108

[7] S. Yang, F. Liao, J. Wu, H. J.P. Timmermans, H. Sun, Z. Gao, A bi-objective timetable optimization model incorporating energy allocation and passenger assignment in an energy-regenerative metro system. Transportation Research Part B 133 (2020) 85–113.

[8] M. Khodaparastan, O. Dutta, M. Saleh, A. A. Mohamed, Modeling and Simulation of DC Electric Rail Transit Systems With Wayside Energy Storage, IEEE Transactions on Vehicular Technology, 68(3) (2019) 2218 - 2228.

[9] R. Barrero, J. V. Mierlo, X. Tackoen, Energy savings in public transport, IEEE Vehicular Technology Magazine 3(3) (2008) 26 - 36.

[10] R. Barrero, X. Tackoen, J. V. Mierlo, Stationary or onboard energy storage systems for energy, in Proceedings of the Institution of Mechanical Engineers, Part F: Journal of Rail and Rapid Transit, 224 (2010) 207–225.

[11] G. Cui, L. Luo, C. Liang, S. Hu, Y. Li, Y. Cao, B. Xie, J. Xu, Z. Zhang, Y. Liu, T. Wang, Supercapacitor Integrated Railway Static Power Conditioner for Regenerative Braking Energy Recycling and Power Quality Improvement of High-Speed Railway System, IEEE Transactions on Transportation Electrification, 5(3) (2019) 702 - 714.

[12] W. Liu, J. Xu, J. Tang, Study on control strategy of urban rail train with on-board regenerative braking energy storage system, IECON 2017 - 43rd Annual Conference of the IEEE Industrial Electronics Society, Beijing, China, (2017) 3924–3929.

[13] F. Ciccarelli, A. Del Pizzo, and D. Iannuzzi, Improvement of energy efficiency in light railway vehicles based on power management control of wayside lithium-ion capacitor storage, IEEE Transactions on Power Electronics, 29(1) (2014) 275–286.

[14] L. Alfieri, L. Battistelli, M. Pagano, Impact on railway infrastructure of wayside energy storage systems for regenerative braking management: a case study on a real Italian railway infrastructure, IET Electrical Systems in Transportation 9(3) (2019) 140 – 149.

[15] F. Meishner, D. U. Sauer, Wayside energy recovery systems in DC urban railway grids, eTransportation, 1, (2019), 100001.

[16] F. Ciccarelli, A. Del Pizzo, and D. Iannuzzi, Improvement of energy efficiency in light railway vehicles based on power management control of wayside lithium-ion capacitor storage, IEEE Transactions on Power Electronics, 29(1) (2014) 275–286.

[17] L. Alfieri, L. Battistelli, M. Pagano, Impact on railway infrastructure of wayside energy storage systems for regenerative braking management: a case study on a real Italian railway infrastructure, IET Electrical Systems in Transportation 9(3) (2019) 140 – 149.
[18] Y. Krim, D. Abbes, S. Krim, M. F. Mimouni, Intelligent Droop Control and Power Management of Active Generator for Ancillary Services under Grid Instability Using Fuzzy Logic Technology. Journal of control Engineering Practice, 81 (2018) 215-230.
[19] Z. Tian, P. Weston, N. Zhao, S. Hillmansen, C. Roberts, L. Chen, System energy optimisation strategies for metros with regeneration, Transp. Res. Part C Emerg. Technol 75 (2017) 120–135.
[20] W. Jefimowski, A. Szelag, The multi-criteria optimization method for implementation of a regenerative inverter in a 3 kV DC traction system, Electric Power Systems Research, 161 (2018) 61–73.
[21] T. Kulworawanichpong, "Multi -train modeling and simulation integrated with traction power supply solver using simplified Newton -Raphson method," Journal of Modern Transportation. 35(6) 241 –251, 2015.
[22] P. Arboleya, I. El-Sayed, B. Mohamed, C. Mayet, Modeling, Simulation and Analysis of On-Board Hybrid Energy Storage Systems for Railway Applications, Energies 2019, 12, 2199.
[23] M. Khodaparastan, A. Mohamed, Modeling and Simulation of Regenerative Braking Energy in DC Electric Rail Systems, IEEE Transportation Electrification Conference and Expo (ITEC), 13-15 June 2018, 10.1109/ITEC.2018.8450133.
[24] N. Haddad, C. Catoire, E. Sourdille, M. Cucchiaro, Integrated solutions for calculus of electromagnetic perturbation of railway track with real traffic conditions, world congress on railway research, may 22-26, 2011, Challenge B: An environmentally friendly railway, 1-4.
[25] P. Pankovits, D. Abbes, C. Saudemont, S. Brisset, J. Pougeta, B. Robyns, Multi-criteria fuzzy-logic optimized supervision for hybrid railway power substations, Mathematics and Computers in Simulation 130 (2016) 236-250.
[26] L. Alfieri, L. Battistelli, M. Pagano, Impact on railway infrastructure of wayside energy storage systems for regenerative braking management: a case study on a real Italian railway infrastructure, IET Electrical Systems in Transportation, 9(3) (2019) 140-149.
[27] B. Milesevic, B. Filipovic-Grcic, I. Uglesic, B. Jurisic, Estimation of current distribution in the electric railway system in the EMTP-RV, Electric Power Systems Research, 162, (2018), 83-88
[28] N. Kouassi, N. Navarro, T. Letrouvé, H. Caron, C. Saudemont, B. Francois, B. Robyns, Dynamic Modelling of Braking Energy Recovered Using a Bi-Directional Power Station on DC Railway Electrical Network, in: IEEE 18th International Power Electronics and Motion Control Conference (PEMC), Budapest, Hungary, (2018) 109–114.
[29] K. Almaksour, H. Caron, N. Kouassi, T. Letrouvé, N. Navarro, C. Saudemont, B. Robyns, Mutual impact of train regenerative braking and inverter based reversible DC railway substation, EPE'19 ECCE Europe conference, Genova, Italy, (2019).
[30] X. Yang, H. Hu, Y. Ge, S. Aatif, Z. He, S. Gao, An Improved Droop Control Strategy for VSC-Based MVDC Traction Power Supply System, IEEE Transactions on Industry Applications, 54(5), (2018) 5173 - 5186.
[31] C. Stackler, N. Evans, L. Bourserie, F. Wallart, F. Morel, P. Ladoux, 25 kV-50 Hz railway power supply system emulation for Power-Hardware-in-the-Loop testings, IET Electrical Systems in Transportation 9(2) (2019) 86-92.
[32] A. Viehweider,, G. Lauss,, L. Felix, Stabilization of Power Hardware-in-the-Loop simulations of electric energy systems, Simulation Modelling Practice and Theory 19(7) (2011) 1699–708. 10.1016/j.simpat.2011.04.001.